

High precision measurement of the hyperfine fields of substitutional and defect associated Cd in single crystalline hcp cobalt

J.G. Correia^{1,2}, N.P. Barradas^{1,†}, A.A. Melo¹ and J.C. Soares¹

1 Centro de Física Nuclear da Universidade de Lisboa, Av. Prof. Gama Pinto 2, 1699 Lisboa Codex Portugal
2 PPE Division, CERN, CH 1211 Genève 23, Switzerland and the ISOLDE Collaboration

ABSTRACT

The hyperfine fields of Cd in single crystalline hcp Co were measured after simultaneous implantation of $^{111\text{m}}\text{Cd}$ and ^{111}In . High statistics measurements could be done separately for each parent isotope combining the e^- - γ and γ - γ PAC techniques. The hyperfine coupling constants $\omega_L(\text{CdCo})=422.8(1)$ Mrad/s and $\omega_0(\text{CdCo})=6.14(11)$ Mrad/s are determined for Cd probes in undisturbed substitutional sites. Several defect associated sites in the hcp Co lattice are clearly seen in the data. Most of the radiation damage created by the ion implantation anneals out at temperatures below 503 K, with only one dominating component surviving at this temperature. This defect is assigned as a probe atom in an interstitial site, surrounded by a vacancy tetrahedron. The corresponding magnetic field and electric field gradient are collinear with the c-axis of the Co lattice, and the respective coupling constants are $\omega_L(\text{defect})=216.7(2)$ Mrad/s and $\omega_0(\text{defect})=45.3(6)$ Mrad/s.

I. INTRODUCTION

The perturbed angular correlation (PAC) technique is a powerful method to study hyperfine fields in solids. In recent years it has in particular been applied extensively to the study of point defects in metals and semiconductors /1,2/. Binding and activation energies for defects have been measured and in some cases the identification of a defect was possible at concentrations down to a few per cent. Another favorable aspect is that different lattice sites can be identified independently of the process of their creation. In favorable cases information on the structure of a lattice defect can also be obtained.

The technique naturally also has various limitations. Beyond the difficulties due to the limited number of probe nuclei with appropriate magnetic or quadrupole moments and suitable lifetimes, there are cases where the technique is insensitive. This is for instance the case when the defect distribution of the near surrounding of the probe nuclei creates vanishing electric field gradients in a cubic lattice. In particular the electric field gradients (efg) of defects or impurities in hcp metals of low symmetry having a c/a ratio near the ideal value $c/a = 1.633$ have not been extensively studied yet for a similar reason. On the other hand, magnetic materials have high internal magnetic fields and the corresponding Larmor frequency ω_L obscures the evaluation of the quadrupole splittings. These can rarely be separated in a clear way from frequency distributions caused by disorder in the near surrounding of the probe.

Extensive studies of defects have been reported for the ferromagnetic fcc metals Ni and Co /3-6/. Little is

known, however, for the hcp phase of Co, which is the stable one below the phase transition to fcc at 704 K. Defects in hcp Co are mobile above the temperature associated with stage III. Resistivity-recovery experiments /7/, however, indicate that the stage III can be shifted to lower temperatures if impurities are present. This technique cannot give information on the defect structure. On the contrary the PAC technique can lead to unique results, if single crystals (SC) are used /8/.

In the present work, point defect studies are reported combining results obtained by implanting both $^{111\text{m}}\text{Cd}$ and ^{111}In in a Co SC. Two different cascades populate the same $5/2^+$ level in ^{111}Cd . Due to the similarity between the hcp and fcc structures which differ only in the stacking of basal planes and the fact that the Co ratio $c/a = 1.623$ is almost equal to the ideal value of $\sqrt{8/3}$, these results can be correlated with the ones obtained for cubic ferromagnetic Ni and fcc Co lattices.

2. EXPERIMENTAL DETAILS

The simultaneous implantation of $^{111\text{m}}\text{Cd}$ and ^{111}In was carried out at the ISOLDE mass separator at CERN /9/. The Cd and In isotopes were produced by the spallation reaction of a 600 MeV proton beam on a molten Sn target. The isotopes are ionized in a discharge plasma ion source and the Cd^+ and In^+ ions then extracted and accelerated electrostatically to an energy of 60 keV. After mass separation the $^{111\text{m}}\text{Cd}$ and ^{111}In ions were implanted into a hcp Co SC at room temperature to a dose of 2×10^{12} at/cm².

[†] Present address: Research Center Rossendorf Inc., POB 510119, 01314 Dresden, Germany

The sample prepared was first used for $e^- \gamma$ and later for $\gamma \gamma$ PAC experiments. First, the $e^- \gamma$ PAC measurement with ^{111m}Cd was performed using a setup with 2.5 ns time resolution, consisting of two β

spectrometers of the Siegbahn type /10/ and two NaI(Tl) detectors arranged in one plane at 90° with each other. The measurements with the ^{111m}Cd probe,

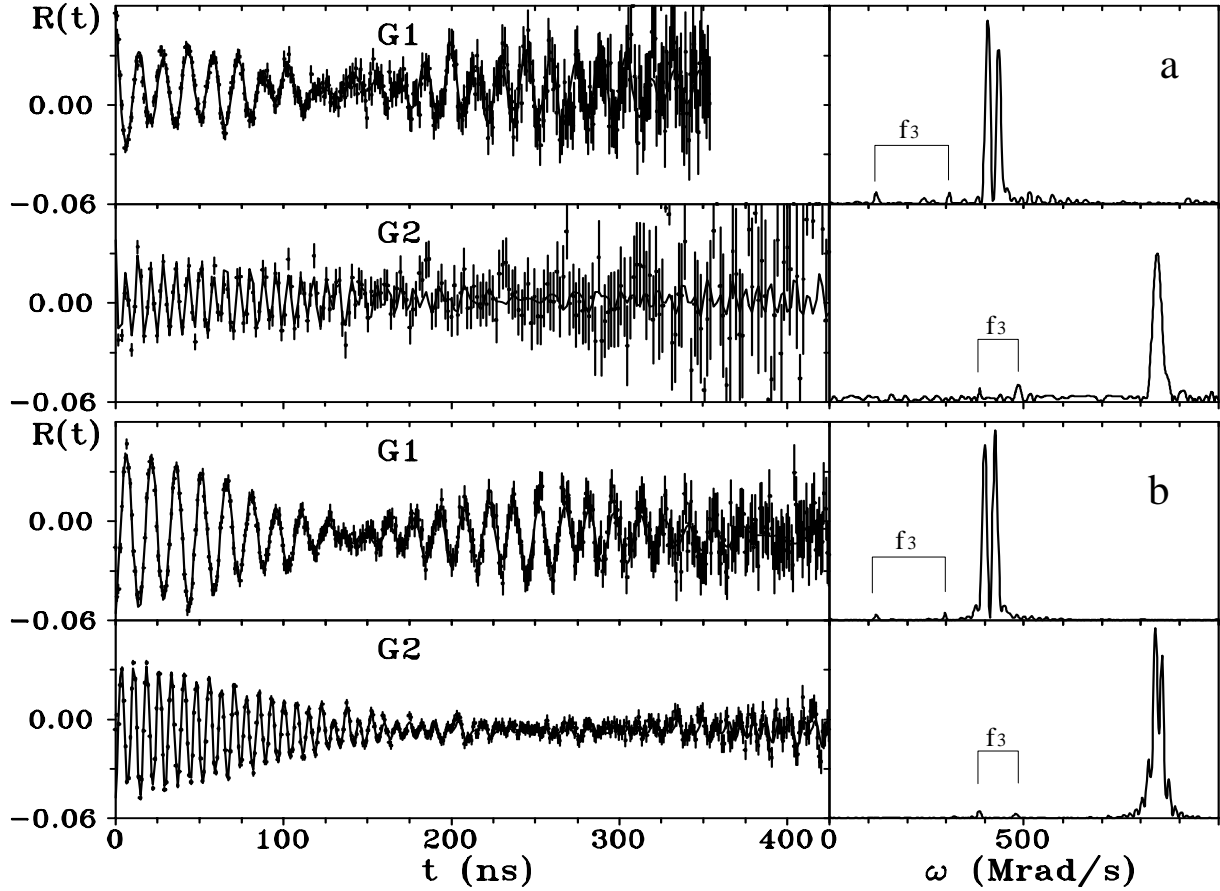


Fig. 1. $R(t)$ functions and corresponding Fourier transforms for a) ^{111m}Cd after room temperature implantation, and b) ^{111}In after annealing at 503 K, for a Co SC in geometries 1 and 2.

co-implanted with ^{111}In , were only possible due to the use of the $e^- \gamma$ PAC technique. The selection of the K-conversion electron from the 150 keV ^{111m}Cd transition, instead of the corresponding gamma ray, excludes any coincidence with the non-separated 170 keV gamma ray from the decay of ^{111}In . After the ^{111m}Cd decay ($T_{1/2}=49$ min), the ^{111}In activity ($T_{1/2}=2.8\text{d}$) could be used for the $\gamma \gamma$ PAC measurements, performed in a four BaF₂ detectors spectrometer with 0.6 ns time resolution. The conventional anisotropy ratio $R(t)$ is formed from the coincidence spectra $N(\theta, t)$ as

$$R(t) = 2 \frac{N(180^\circ, t) - N(90^\circ, t)}{N(180^\circ, t) + 2N(90^\circ, t)} \quad (1)$$

A theoretical $R(t)$ function, formally equal to the experimental one, is calculated numerically /8/ and fitted to the data, taking into account the full Hamiltonian and all the terms up to G_{44} for the combined magnetic and electric hyperfine interaction in the ferromagnetic hcp Co SC. In the calculation we

assume that different fractions f_i of probe nuclei are localized at different lattice sites feeling different hyperfine fields. For each fraction, the Larmor $\omega_L = -\frac{\mu B_{hf}}{\hbar I}$ and the quadrupole $\omega_0 = \frac{6eQV_{zz}}{4I(2I-1)\hbar}$ frequencies are derived, where B_{hf} is the magnetic hyperfine field of fraction i , V_{zz} is the main component of the efg tensor, and μ and Q are the magnetic dipole and electric quadrupole moments of the probe nucleus.

No external magnetic field is applied to orient the magnetic domains in the Co SC. The spins of the Co lattice below 510 K are aligned along the c-axis /11/, which is also the direction of the lattice V_{zz} . In order to derive with the highest accuracy the frequencies and respective amplitudes for each fraction of probe nuclei in a well characterized lattice site, experiments at two different geometries were performed. In geometry G1, the c-axis of the SC was oriented in the detectors plane at an angle of 45° with the detectors, and in geometry G2 it was perpendicular to the

detectors plane. For a collinear interaction, the observed frequencies are $\omega_L \pm 2\omega_0$ with minor $\omega_L \pm \omega_0$ amplitudes for G1, and $2\omega_L \pm \omega_0$ for G2. The frequencies are directly visible in the Fourier transforms of the R(t) spectra, and are used to determine a first guess in the fit.

3. RESULTS AND DISCUSSION

In fig. 1a and b are shown the R(t) functions and corresponding Fourier transforms measured in geometries G1 and G2, for the same Co SC, using the e^- - γ and γ - γ cascades in the decay of the ^{111m}Cd and

	^{111m}Cd 295 K	^{111m}Cd 503 K	^{111}In 295 K
ω_L^1 (Mrad/s)	422.8(2)	398.6(4)	422.9(1)
ω_0^1 (Mrad/s)	6.18(10)	5.71(27)	6.10(9)
δ_1 (Mrad/s)	0	0	0
f_1 (%)	15.3(3)	22.2(7)	5.9(2)
ω_L^2 (Mrad/s)	422.8(2)	398.6(4)	422.9(1)
ω_0^2 (Mrad/s)	6.18(10)	5.71(27)	6.10(9)
δ_2 (Mrad/s)	194(8)	179(8)	6(1)
f_2 (%)	18(2)	15(2)	19(1)
ω_L^3 (Mrad/s)	216.5(8)	196(2)	216.8(6)
ω_0^3 (Mrad/s)	45.1(4)	41.3(9)	46.1(7)
δ_3 (Mrad/s)	0	0	0
f_3 (%)	3.2(3)	4.4(6)	3.0(3)

Table 1. Main parameters of the hyperfine interaction of ^{111}Cd in hcp Co.

^{111}In isotopes, respectively. The SC has been annealed at 503 K between the experiments with ^{111m}Cd and ^{111}In , which explains the difference in the amplitudes of the respective R(t) functions. The opposite sign is due to the different multipolarity of the 150 and 170 keV first transition of the e^- - γ and γ - γ cascades, respectively.

For each probe, the results of both geometries were fitted consistently, with the same values for the interaction frequencies, the angles between hyperfine fields and the fractions f_i of probes. The perfect compatibility between the fits leads to a maximum precision for the determination of the values of the hyperfine fields and their directions. The parameters derived are given in table 1, which also include the results from an experiment with ^{111m}Cd done at 503 K (not shown). The error bars were calculated during the fit procedure, and do not include a $\leq 1\%$ time calibration error. No sign of the fcc phase was found.

The first observation is the maximum amplitude of the R(t) function, where after annealing only 40% and 30% of the expected anisotropy value is observed, respectively for the ^{111m}Cd and ^{111}In experiments. Previous experiments of ^{111}In implanted in fcc SC Co thin films /6/ and in hcp Co thin films /12/ show the

same effect. In spite of the defect recovery seen at 503 K, the majority of the Cd and In atoms is interacting with large distributions of hyperfine fields, probably due to vacancy clusters not dissociating at 503 K ^{111}In is well known to be a powerful vacancy catcher. Vacancies are mobile at room temperature in Co and the formation of vacancy clusters cannot be avoided /7/. The resulting combined hyperfine interaction must lead to a spin rotation too fast to be resolved.

The main amplitudes seen correspond to substitutional Cd in hcp Co, and the interaction frequencies derived are $\omega_L=422.8(2)$ Mrad/s and $\omega_0=6.18(10)$ Mrad/s, from the fits to the ^{111m}Cd data and $\omega_L=422.9(1)$ and $\omega_0=6.10(9)$ Mrad/s using ^{111}In . Both fields are along the c-axis. These high precision values of the frequencies agree with previous data of Barradas et al /8/ and Lindgren et al /13/ obtained in SC and polycrystals respectively. The relevance of using SC for defect studies comes from the unique possibility to determine simultaneously the direction and value of the fields. The characterization of Cd-hcp Co associated defects becomes possible, and is a first step to investigation more complex systems, such as Co based multilayers and thin films.

In order to fit the high statistics data of fig. 1, we have to introduce two fractions, f_1 and f_2 , with the same values for the magnetic and quadrupole frequencies, but with different magnetic field distributions, here assumed to have Lorentzian shape. For the first it is $\delta=0$ Mrad/s, while for the second, $\delta=179$ Mrad/s after annealing for ^{111m}Cd and $\delta=6$ Mrad/s for ^{111}In , leads to the attenuation observed in the measurements. Far away defects or a lattice distortion can be responsible for that, and we assume that the total amount of Cd atom probes in substitutional sites is f_1+f_2 . In this experiment, where both isotopes were implanted simultaneously, we should expect the same density of defect cascades independently of the relative dose of ^{111m}Cd and ^{111}In . The difference of about 12% in f_1+f_2 for the two probes, measured after annealing at 503 K, shows evidence of a smaller capability of Cd to act as a defect trapping center inside the Co matrix, relatively to In.

The small amplitude fraction f_3 , has a higher quadrupole splitting centered in a lower magnetic frequency, leading to fully resolved observable frequencies. This allowed to determine, in spite of the small value of the fraction, that both the magnetic field and the efg are along the c-axis of the SC.

At 503 K the f_3 value increases slightly. Taking into account that an In-vacancy ($\text{In}_i\text{-V}_4$) complex has been observed in both Ni and fcc Co lattices /3-6/ showing a similar behavior we assign this frequency to this defect, which can be formed in the following way: an In (Cd) atom in a substitutional lattice site traps a tri-vacancy and relaxes to the tetrahedral

interstitial lattice site in the hcp lattice. In the formation of this complex only two basal planes are involved, ignoring further relaxation phenomena: the one with the original tri-vacancy, and the other with

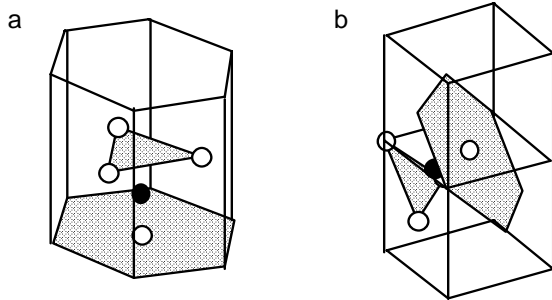


Fig. 2. The In_i-V_4 complex in the a) hcp and b) fcc structures. The black and white circles are the interstitial atom and the vacancies, respectively.

the In (Cd) atom. The interlayer distance is almost the same due to the almost ideal c/a ratio, and so no difference between the hcp and fcc stackings can be seen at the two layer level, and therefore the same defect can exist in both hcp and fcc Co structures, as shown in fig. 2.

In a fcc structure the In_i-V_4 complex has cubic symmetry and hence no efg can be measured. On the contrary in the hcp structure it has a rather large efg. The efg due to the hcp Co lattice, V_{zz}^{lat} , was calculated by the point charge model for the substitutional and In_i-V_4 configurations. We used the semi-empirical law

$$V_{zz}^{eff} = (1-\gamma)(1-K) V_{zz}^{lat}, \quad (2)$$

where V_{zz}^{eff} is the measured efg, γ is the antishielding Sternheimer factor accounting for core polarization, and K is an empirical value accounting for a proportionality between the electronic and lattice contributions to the efg, which lies generally between 2 and 4 /14/. For the substitutional configuration, V_{zz}^{lat} (subs) was calculated with the Das and Pomerantz exact formula /15/, and V_{zz}^{eff} (subs) is the experimental value. We obtain $K=2.18$ (19). Using the point charge model for the In_i-V_4 unrelaxed configuration, we obtain $V_{zz}^{lat}(In_i-V_4)=6.3(6) \times 10^{17}$ V/cm², yielding $V_{zz}^{eff}(In_i-V_4)=-224(42) \times 10^{17}$ V/cm², which compares well with $V_{zz}^2=238(37) \times 10^{17}$ V/cm². Although the model used in the calculation is rather simple, it shows that a non-zero efg of the correct order of magnitude is indeed expected for the In_i-V_4 configuration in hcp Co.

This defect complex is observed in both ¹¹¹In and ^{111m}Cd implanted samples, with similar small fractions. It has also been observed in fcc Ni and Co with the ¹¹⁹Sn probe /16/. These three probes have similar ionic radius, and they are about 0.2 Å larger

than the ionic radius of Co, which leads to the known preferential trapping of vacancies by oversized impurities /17/.

Finally, it was not possible to identify clearly the additional frequencies seen in the data taken after implantation, which disappear with annealing. These frequencies and their amplitudes cannot be explained by a c -axis efg direction. Although many attempts have been done, no unique solution could be found due to the small amplitude, about 2% of the probe nuclei.

4. CONCLUSIONS

The hyperfine fields of Cd in hcp SC Co were measured after simultaneous implantation of ^{111m}Cd and ¹¹¹In. High statistics measurements could be done separately for each parent isotope combining the e^- - γ and γ - γ PAC techniques. The determination of the strength and orientation of the hyperfine fields that characterize each complex were possible by measuring the combined interaction in two different orientations of the hcp Co SC, without using any external field.

Point defects in a ferromagnetic non-cubic lattice were studied, to our knowledge, for the first time. One defect has been characterized in terms of its magnetic and electric interaction frequencies, orientation, and annealing behavior, and related to the In_i-V_4 specific vacancy configuration.

ACKNOWLEDGMENTS

This work has been supported by JNICT under contracts CA/89/1, STRIDE/CERN/C/CA/62/91 and STRD/C/CA/982/92. J.G.C. and N.P.B. acknowledge grants from Program CIÊNCIA.

REFERENCES

- /1/ E.N. Kaufman and R. Vianden, Rev. Mod. Phys. 51 (1979) 161.
- /2/ Th. Wichert and E. Recknagel, in *Microscopic Methods in Metals*, ed. by U. Gonser (Springer, Berlin 1986) p. 317.
- /3/ F. Pleiter and C. Hohenemser, Phys. Rev. B 25 (1982) 106.
- /4/ C. Allard, G.S. Collins and C. Hohenemser, Phys. Rev. B 32 (1985) 4839.
- /5/ F. Raether, G. Weyer, K. P. Lieb and J. Chevallier, Phys. Lett. A 131 (1988) 471.
- /6/ G. Weyer, Hyp. Int. 51 (1989) 901.
- /7/ S. Habtetsion, H. J. Blythe, F. Dworschak and U. Dedek, J. Phys.: Cond. Matt, 1 (1989) 9519.
- /8/ N.P. Barradas, M. Rots, A.A. Melo and J.C. Soares, Phys. Rev. B 47 (1993) 8763.
- /9/ B.W. Allardyce and H. Ravn, Nucl. Instr. and Meth. B26 (1987) 112.

- /10/ P. Kleinheinz, L. Samuelsson, R. Vukanovic and K. Siegbahn, Nucl. Instr. and Meth. 32 (1965) 1.
- /11/ D.M. Paige, B. Szpunar and B.K. Tanner, J. Magn. and Magn. Mat. 44 (1984) 239.
- /12/ N.P. Barradas, H. Wolters, A.A. Melo, J.C. Soares, M.F. da Silva, M. Rots, J.L. Leal, L.V. Melo and P.P. Freitas, J. Appl. Phys. 76 (1994) 6537.
- /13/ B. Lindgren, S. Bedi and R. Wäppling, Phys. Scr. 18 (1978) 26.
- /14/ R.S. Raghavan, E.N. Kaufmann and P. Raghavan, Phys. Rev. Lett. 34 (1975) 1280.
- /15/ T.P. Das and M. Pomerantz, Phys. Rev. 123 (1961) 2070.
- /16/ K.B. Nielsen, E. Danielson, J.W. Peterson, M. Søndergaard and G. Weyer, Hyp. Int. 35 (1987) 643.
- /17/ L. Thomé and H. Bernas, Hyp. Int. 5 (1978) 361.